

Inclusive cross section and correlations of fully reconstructed jets in $\sqrt{s_{NN}} = 200$ GeV/c Au+Au and $p+p$ collisions

Mateusz Płoskoń for the STAR Collaboration

*Lawrence Berkeley National Laboratory
1 Cyclotron Road, Berkeley, CA 94720, USA*

Abstract

We present an experimental study of full jet reconstruction in the high multiplicity environment of heavy ion collisions, utilizing $\sqrt{s_{NN}} = 200$ GeV/c $p+p$ and central Au+Au data measured by STAR. Inclusive differential jet production cross sections and ratios are reported, as well as high p_T hadron+jet coincidences.

1. Introduction

Measurements of jet quenching via single and di-hadron observables [1] have provided initial estimates of the energy density of the hot QCD medium generated in high energy nuclear collisions. However, such observables suffer from well-known biases and are limited in their sensitivity [2]. Fully reconstructed jets will enable an unbiased exploration of quenching, including new observables of energy flow within jets whose theoretical description is not dependent upon the modeling of hadronization.

Full jet reconstruction is difficult in the heavy-ion collision environment. Attempts to suppress background via seeded algorithms or the introduction of a modest cut on hadron p_T in the jet reconstruction results in a population biased against quenched jets [3]. Our emphasis in this analysis is to minimize such biases. We apply the minimum cuts possible within the STAR acceptance ($p_T > 0.2$ GeV/c) and use seedless algorithms in both $p+p$ and Au+Au collisions. We confront the challenging problem of high-density backgrounds by applying recently developed jet finding and background correction algorithms of the FastJet package [4]. We report inclusive jet cross-sections in $\sqrt{s_{NN}} = 200$ GeV/c $p+p$ and 10% most central Au+Au collision, using two resolution scales ($R = 0.2$ and $R = 0.4$). We report their ratios, jet R_{AA} , and hadron-jet correlations.

The results presented in these proceedings differ quantitatively in two respects from those presented at the conference, though all qualitative conclusions are unchanged. For $p+p$ collisions, full correction for the jet trigger bias has now been applied, whereas an approximation was used previously, resulting in an increase in the central value of the cross section for $p_T^{jet} < 30$ GeV/c and corresponding decrease in R_{AA} . For Au+Au collisions, the study of simulated (Pythia) jets embedded in Au+Au background events resulted in a revision of the parameterization of background fluctuations. We correct the overall scaling error which for narrow jets ($R = 0.2$) results in a corresponding increase of up to a factor 3 in the inclusive cross section.

26 **2. Data sets, algorithms and procedures**

27 For $p+p$ collisions we use 12 pb^{-1} , recorded in Run 6 with a jet patch trigger, requiring
 28 $> 7.6 \text{ GeV}/c$ in a fixed BEMC region of dimensions $\Delta\phi \times \Delta\eta = 1 \times 1$. For central Au+Au
 29 collisions we use 7.6M most central events ($\sigma/\sigma_{\text{Geom}} = 10\%$), recorded in Run 7 with a minimum
 30 bias trigger. Jet reconstruction in both heavy-ion and $p+p$ collisions utilizes the kt and anti-kt
 31 algorithms from the FastJet package [4]. The two algorithms have different sensitivity to heavy-
 32 ion background. The energy recombination scheme is used for tracks and calorimeter towers,
 33 which are assigned zero mass. Jet candidates are found utilizing two resolution parameters $R =$
 34 0.2 and $R = 0.4$, within acceptance $|\eta^{\text{Rec}}| < 0.6$. Fragmentation biases are minimized through the
 35 minimal cuts ($p_T^{\text{Track|Tower}} > 0.2 \text{ GeV}/c$ and $|\eta^{\text{Track|Tower}}| < 1$). BEMC towers matched with one or
 36 more TPC tracks are removed from analysis.

37 Background subtraction is applied event-wise via $p_T^{\text{Rec}} = p_T^{\text{Candidate}} - \rho \cdot A$, where ρ mea-
 38 sures p_T -weighted density of background in an event and A is the measured jet area [4]. We
 39 define signal jets with $p_T^{\text{rec}} > 0$ and background jets with $p_T^{\text{rec}} \leq 0$. For central Au+Au collisions,
 40 $\rho \approx 75 \text{ GeV}/c$ per unit area within $-0.6 < \eta < 0.6$. The term $\rho \cdot A$ is the most probable value of the
 41 background underlying the signal jet. Fluctuations around this value are characterized by Gaus-
 42 sian distribution with width of σ^{bg} , which is applied in an unfolding procedure to correct the in-
 43 clusive spectrum. The value of σ^{bg} extracted from the distribution of background jets reproduces
 44 the spectrum distortion of Pythia jets embedded into central Au+Au events only for $R = 0.4$, but
 45 not for $R = 0.2$. This may be related to the non-Gaussian nature of the background fluctuations;
 46 the Pythia embedding is more sensitive to the upwards fluctuations, which are predominantly
 47 responsible for the spectrum distortion. We therefore utilize in these proceedings the correction
 48 factors extracted from embedded Pythia, $\sigma^{\text{bg } R=0.4} = 6.8 \text{ GeV}/c$ and $\sigma^{\text{bg } R=0.2} = 3.7 \text{ GeV}/c$. This
 49 choice results in an increase of a factor ~ 3 in the inclusive jet cross-section for $R = 0.2$.

50 Prior to the unfolding procedure the signal jet spectrum is corrected for “false”-jet yield,
 51 defined as the signal in excess of the background model from random association of uncorrelated
 52 soft particles. This is estimated by running the jet finders on a randomized Au+Au event, with
 53 jet-leading particles removed.

54 The jet energy correction for tracking inefficiency, approximated in this analysis to be p_T^{Track}
 55 independent, is 8% in $p+p$ and 12% in Au+Au, and for unobserved neutral energy (neutrons,
 56 K_0^L) it is 5% in both systems. The total instrumental jet energy resolution ($\sigma^{\text{Resol}}(E)/\langle E \rangle \approx 20\%$
 57 [5]) is corrected by unfolding. The systematic uncertainty on the jet energy scale, shown in all
 58 figures as the vertical yellow band, is dominated by the uncertainties on the BEMC calibration
 59 (5%), unobserved jet energy (3%), and charged momentum resolution (2%). Solid lines represent
 60 systematic uncertainty on the jet yield in Au+Au due to background fluctuations.

61 **3. Inclusive cross-sections and ratios**

62 Figure 1 presents the inclusive differential cross-sections of fully reconstructed jets from
 63 $p+p$ and 10% most central Au+Au collisions at $\sqrt{s_{NN}} = 200 \text{ GeV}/c$. The reconstructed jet
 64 yields extend in p_T^{jet} beyond $50 \text{ GeV}/c$. The $p+p$ measurement agrees within uncertainties with
 65 the published cross-section (mid-point cone, $R = 0.4$) [6].

66 Figure 2, left panel, shows R_{AA}^{jet} , the ratio of the jet yield in Au+Au over the binary collision-
 67 scaled jet yield in $p+p$. For unbiased jet reconstruction this ratio is expected to be close to unity,
 68 within possible deviations due to initial state effects. We find R_{AA}^{jet} for $R = 0.4$ compatible with
 69 unity with the large uncertainties. R_{AA}^{jet} for $R = 0.4$ is significantly larger than R_{AA} of hadrons

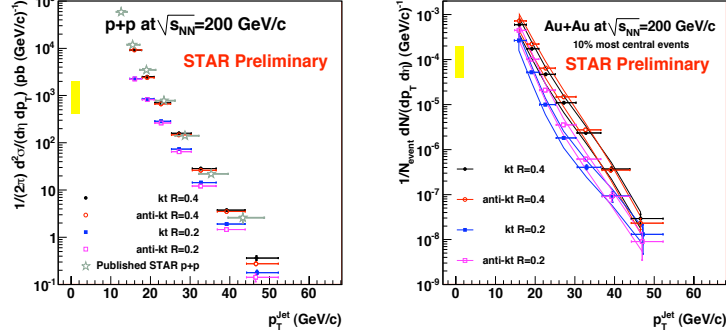


Figure 1: Inclusive jet cross-sections in $\sqrt{s_{NN}} = 200$ GeV/c $p+p$ (left) and $Au + Au$ collisions (right) (kt and anti-kt, R : 0.2 and 0.4). Error bands described in the text. Published $p+p$ data are from [6].

70 for $p_T < 20$ GeV/c ($R_{AA}^{\text{hadron}} \approx 0.2$). R_{AA}^{Jet} for $R = 0.2$ is markedly below R_{AA}^{Jet} for $R = 0.4$. Note
 71 the significant differences between kt and anti-kt algorithms, possibly arising from their different
 72 response to the heavy-ion background.

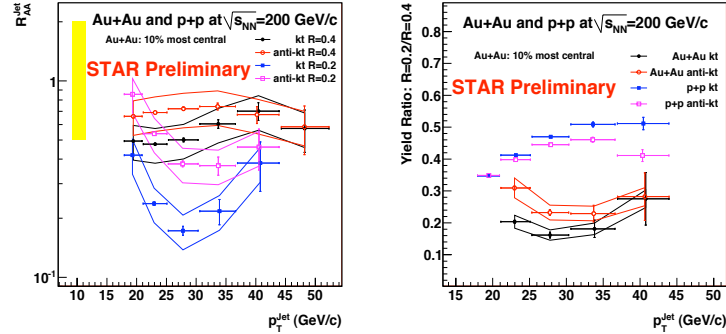


Figure 2: Ratios of inclusive jet cross-sections in $\sqrt{s_{NN}} = 200$ GeV/c $p+p$ and $Au + Au$ collisions (kt and anti-kt, R : 0.2 and 0.4). *Left*: Jet R_{AA} . *Right*: Ratio of cross-sections $R = 0.2/R = 0.4$ for each system.

73 Fig. 2, right panel, shows the ratio of jet yield for $R = 0.2$ over that for $R = 0.4$, separately
 74 for $p+p$ and $Au+Au$ collisions. Several jet energy scale systematic uncertainties cancel in this
 75 ratio. For $p+p$ collisions the ratio increases with p_T^{jet} , consistent with a Pythia calculation but
 76 not a recent NLO calculation [7]. The ratio is strongly suppressed for central $Au+Au$ relative to
 77 $p+p$ collisions, indicating substantial broadening of the jet structure in heavy ion collisions.

78 4. Hadron-jet coincidences

79 We study the correlation of high-pt trigger particles (BEMC cluster with $p_T > 6$ GeV/c) with
 80 a recoiling jet (matched in away-side azimuth within $|\Delta\phi| < 0.4$), comparing central $Au+Au$
 81 and $p+p$ collisions. In $Au+Au$ this exploits the geometric bias of high-pt hadron production [2]

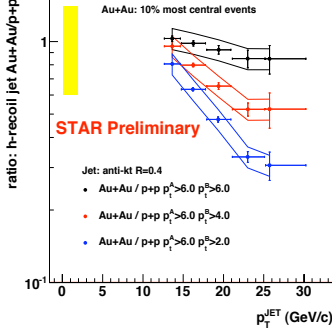


Figure 3: Ratios of hadron-jet conditional yields for three selections of the leading particle of the recoil jet reconstructed in 10% most central $Au + Au$ collisions and $p+p$ collisions. Jets were reconstructed with anti-kt algorithm with $R = 0.4$ and correlated at $\Delta\phi \approx \pi$ with a leading “high tower trigger” (dominated by π^0).

82 due to quenching, which maximizes the path length in matter of the recoiling jet. Additional
 83 geometric bias can be applied by varying the p_T thresholds of the leading hadron in the recoil
 84 jet. The recoil-jet spectra have been corrected for the “false”-jet contamination, described above.
 85 Additional uncorrected background may be due to multiple hard interactions in one $Au+Au$
 86 collision. The correlation yields are normalized to the number of “trigger di-hadrons”.

87 Figure 3 shows the ratio of conditional jet yields ($Au+Au/p+p$) vs. jet p_T , for various recoil
 88 jet leading particle thresholds. The strongly exclusive requirement of two back-to-back high-pt
 89 particles biases in $Au+Au$ towards jets with little interaction, whereas a more relaxed condition
 90 permits more interacting jets. The ratio for the “high- p_T ” selection is consistent with unity,
 91 indicating that in $Au+Au$ collisions we reconstruct the same jet population per di-hadron trigger
 92 as in $p+p$ collisions. For the “low- p_T ” selection, on the contrary, the ratio is below unity and
 93 significantly dropping as a function of p_T^{Jet} , indicating substantial redistribution of jet energy in
 94 heavy-ion collisions. Related di-jet correlation studies are presented in [8].

95 5. Summary

96 We have presented the inclusive cross-section of fully reconstructed jets in $p+p$ and $Au+Au$
 97 collisions at $\sqrt{s_{NN}} = 200$ GeV/c with two different jet algorithms and with two different res-
 98 olution parameters $R = 0.2$ and $R = 0.4$. While R_{AA}^{jets} for $R = 0.4$ is compatible with unity
 99 within large uncertainties, more discriminating measurements of the inclusive cross section as a
 100 function of resolution parameter and hadron+jet correlations indicate strong broadening of the
 101 jet structure in heavy-ion collisions.

102 References

- 103 [1] J. Adams et al. [STAR Collaboration] Phys. Rev. Lett. 91, 072304 (2003), J. Adams et al. [STAR Collaboration]
 104 Phys. Rev. Lett. 97, 162301 (2006), S. S. Adler et al. [PHENIX Collaboration] Phys. Rev. C69, 034910(2004)
 105 [2] T. Renk, Phys. Rev. C **78**, 034904 (2008) [arXiv:0803.0218 [hep-ph]].
 106 [3] S. Salur [STAR Collaboration], Eur. Phys. J. C **61**, 761 (2009) [arXiv:0809.1609 [nucl-ex]].
 107 [4] M. Cacciari, G. P. Salam and G. Soyez, JHEP 0804 (2008) 005 [arXiv:0802.1188 [hep-ph]]
 108 [5] H. Caines [STAR Collaboration], arXiv:0907.3460 [nucl-ex].
 109 [6] B. I. Abelev et al. [STAR Collaboration] Phys. Rev. Lett. 97 (2006) 252001
 110 [7] W. Vogelsang, private communication (2009)
 111 [8] E. Bruna [STAR Collaboration], arXiv:0907.4788 [nucl-ex].